

Microstructure and properties of crystallized melt-spun $\text{Ti}_{50}\text{Ni}_{25}\text{Cu}_{25}$ ribbons after current-driven thermal cycling

P. Schloßmacher, H. Rösner, A.V. Shelyakov¹, G. Gomasca² and G. Airoidi³

Forschungszentrum Karlsruhe, Institute for Materials Research I, P.O. Box 3640,
76021 Karlsruhe, Germany

¹ Department of Solid State Physics, Moscow Engineering Physics Institute,
Kashirskoe Shosse 31, 115409 Moscow, Russia

² INFN, Dipartimento di Fisica, Università di Milano, Via Celoria 16, 20133 Milano, Italy

³ Dipartimento di Scienza dei Materiali, Via R. Cozzi 53, 20125 Milano, Italy

Abstract. The influence of thermal cycling driven by electrical current under a small and constant applied stress of 50 MPa on martensitic transformation, microstructure and electrical resistance of crystallized melt-spun ribbons of a $\text{Ti}_{50}\text{Ni}_{25}\text{Cu}_{25}$ (at.%) shape memory alloy is investigated. Cycled specimens and uncycled ones as a reference are characterized by various methods like differential scanning calorimetry, X-ray diffraction, transmission electron microscopy, and electrical resistance. After thermal cycling DSC curves during cooling exhibit two transformation peaks whereas the reverse transformation proceeds in only one step. The separation of the two peaks and also their maximum remains stable during cycling but the peak shapes become broader. The reason for the two-stage transformation is found in a crystalline surface layer already present in the as-spun state. A heat treatment between 700°C and 800°C for 600s is able to recrystallize the surface layer. Only minor changes of the microstructure due to current-driven thermal cycling could be observed. The average grain size is about 500 nm in both cycled and uncycled specimens. A few plate-like precipitates are present created during the crystallization process. Twins are frequently observed. Dislocations, however, are never observed not even in the cycled specimens.

1. INTRODUCTION

TiNi-based shape memory alloys (SMAs) are by far the most widely applied SMAs due to their excellent shape memory behavior and superelastic properties. For actuators, thin wires and melt-spun ribbons are of great interest. TiNiCu SMA melt-spun ribbons offer transformation temperatures close to bulk material and a small thermal hysteresis [1,2]. Not too many studies were undertaken up to now in order to investigate the long term stability e.g. under thermal cycling. Recently, a method and first results of current-driven thermal cycling under a constant applied stress was described [3,4].

In this study the influence of current-driven thermal cycling under an applied stress of 50 MPa on the transformation behavior and the microstructure is investigated. A crystalline surface layer present already in the as-spun state was found to be responsible for a uncommon second transformation peak in a differential scanning calorimetry (DSC) experiment. The nature of this layer and its connection to the second DSC peak is described in detail and a heat treatment is given to recrystallize this layer. Electrical resistivity related results are presented in another contribution [5].

2. EXPERIMENTAL

A ribbon with a composition of $\text{Ti}_{50}\text{Ni}_{25}\text{Cu}_{25}$ (at.%) was produced by a single-roller melt-spinning technique [2] from a pre-synthesized ingot. The ribbon is about 1.7 mm in width and about 40 μm in thickness. In order to achieve a fully crystalline state the ribbons were heat treated at 500°C for about 300 s (5 minutes) in vacuum. After the annealing time the ribbons were cooled down in vacuum in about 240 s to 400°C and another 900–1200 s to 200°C, respectively.

For thermal cycling the ribbon was cut into several pieces about 180–190 mm in length. Water-cooled grips with built-in electrical contacts were used to fix a constant temperature at the contacts. A gauge length of 100–110 mm was chosen. Moreover, the whole set-up was sheltered from air draughts. Thermal cycling itself was performed by repeated current-driven heating to transform into the austenite phase and subsequent passive cooling back to the martensite phase under a constant stress of 50 MPa using an

experimental procedure described in detail elsewhere [3]. The choice of 50 MPa is related to previous results [3,4] and corresponds to a minimum hysteresis width in strain vs. normalized electrical resistance curves. For further investigations two conditions with 100 cycles ("AN09", "AN02") and 5230 cycles ("AN07"), respectively, were selected. Parts of the ribbons outside the grip were taken as uncycled ones for comparison.

The transformation behavior of the crystallized ribbons after cycling as well as in the uncycled state was investigated by differential scanning calorimetry (DSC). A Netzsch DSC cell 204 together with a TASC 414/3 A controller was applied. Two thermal cycles between -100°C and $+130^{\circ}\text{C}$ were measured for each specimen by a heating/cooling rate of 0.1667 K/s (10 K/min).

X-ray diffractometry (XRD) was performed with a SIEMENS D500 diffractometer using $\text{Cu-K}\alpha$ radiation ($\lambda = 0.15418\text{ nm}$, $U = 45\text{ kV}$, $I = 40\text{ mA}$) in Bragg-Brentano geometry. $\text{Cu-K}\beta$ radiation was successfully suppressed by a thin Ni foil placed between the two collimating apertures on the detector side. The temperature inside the x-ray chamber was measured to be $33 \pm 1^{\circ}\text{C}$ during a measurement. The specimens, about 35 mm in length, were fixed by plasticine. The software package DIFFRACT AT, Release 3.3 (©Siemens, 1993), was used for evaluation of the data and for calculating the X-ray penetration depths.

Transmission electron microscopy (TEM) was carried out using a Philips CM 30 ST at 200 kV equipped with a double-tilt specimen holder (Gatan, model 646) and an energy-dispersive X-ray spectrometer (Noran, high-purity Germanium detector). TEM specimens were prepared electrochemically using a solution of nitric acid (1 part) and methanol (2 parts) and applying a voltage of $13\text{--}16\text{ V}$ at a temperature of -25°C in a Struers Tenupol 3 electropolishing device equipped with a Haake F3 cooling system.

3. RESULTS AND DISCUSSION

3.1 Transformation behavior

The DSC curves of the first two heating and cooling cycles of specimen "AN09" after 100 current-driven thermal cycles is shown in Fig. 1(a). For comparison, a portion of the same part of the ribbons positioned outside the grips and therefore not thermal cycled is displayed in Fig. 1(b). The difference in specimen weight between cycled and uncycled state is due to the amount of ribbon available. After 100 thermal cycles under the applied stress of 50 MPa the martensitic transformation clearly shows two peaks whereas the reverse transformation observed during the heating cycle exhibits only a single peak. The DSC data of the uncycled "reference" material, however, displayed in Fig. 1(b), show evidence for two peaks in both cooling and heating. The common feature of Fig. 1 (a) and (b) is that the peaks of the first two heating and cooling cycles for each specimen, the cycled one and the uncycled one, are almost identical. There is only one difference in the martensitic transformation of the uncycled material of AN07 which exhibits two peaks in the first cooling cycle and only a peak with a shoulder on the high-temperature side in the second cycle as can be seen in Fig. 1(b).

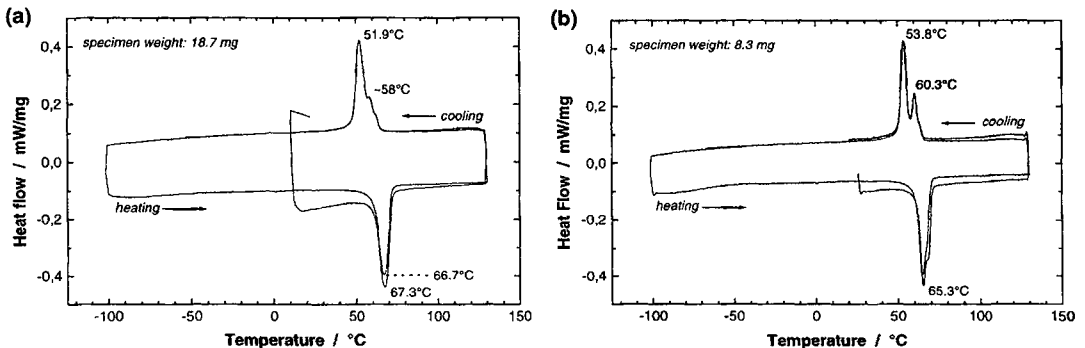


Figure 1: DSC curves of specimen "AN09" after 100 cycles (a) and uncycled (b), i.e. without any cycling, for reference.

treated during the same procedure as for "AN09" and was also thermal cycled for 100 times under a stress of 50 MPa. Thus, "AN02" and "AN09" are nominally identical.

The optical micrograph of the cross-section (perpendicular to the length of the ribbon) of "AN02" is displayed in Fig. 3(a). A surface layer about 8–11 μm in thickness is visible at the so-called "free" surface. In the single-roller melt spinning technique the melt is ejected through a nozzle onto the surface of a fast rotating Cu wheel and is quenched into ribbon shape. This ribbon has two surfaces: one which was in contact with the Cu wheel, called the "wheel" surface, and the opposite one, which we call the "free" surface. Since crystallization starts from the Cu wheel the material at the "free" surface solidifies at last and, therefore, with the lowest cooling rate. The existence of a surface layer leads to the assumption that directly after solidification, i.e. in the as-spun state, this surface layer is already present.

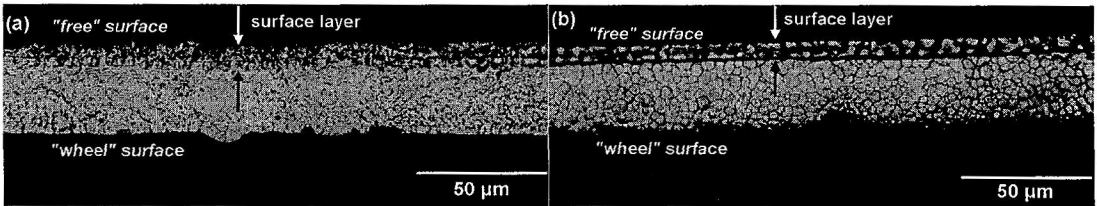


Figure 3: Optical micrographs of metallographic cross-sections of "AN02" after 100 cycles (a) [comparable to "AN09"] and of the as-spun ribbon (b) without any heat treatment.

Consequently, a cross-section of the ribbon used throughout this study but in the as-spun state was prepared and its optical micrograph is presented in Fig. 3(b). Again, a surface layer is visible at the "free" surface, slightly smaller in thickness, about 7–8 μm , compared to the crystallized ribbon shown in Fig. 3(a). Below this layer crystalline grains can be seen a couple of microns in diameter. The crystalline nature seems to extend nearly through the entire thickness of the ribbons to the "wheel" surface.

In order to check the nature of the above mentioned surface layers XRD profiles were recorded from both surfaces of the as-spun and also of the crystallized ribbons. Fig. 4 presents in (a) the XRD profiles of crystallized specimen "AN02" as a function of the scattering angle 2θ in the range from 25° to 65° . The upper plot shows the XRD profile taken from the "free" surface. Only peaks of the B19 martensite phase are observed. Especially in the 2θ range around 42° no XRD peaks are visible as a result of a strong (100) texture of the surface layer. The calculation of the penetration depth of Cu- K_α radiation into $\text{Ti}_{50}\text{Ni}_{25}\text{Cu}_{25}$ by the SIEMENS software results in 4 μm for $2\theta=25^\circ$ and 10 μm for $2\theta=65^\circ$. Therefore, more or less the entire XRD signal stems from the surface layer which consequently consists of textured B19 martensite. The lower plot showing the XRD profile of the "wheel" surface from the same part of the ribbon "AN02". These XRD data exhibit the expected feature of a B19 martensitic structure. The lattice parameters of the martensite lattice are determined to $a = 0.2913 \text{ nm}$, $b = 0.4298 \text{ nm}$ and $c = 0.4524 \text{ nm}$.

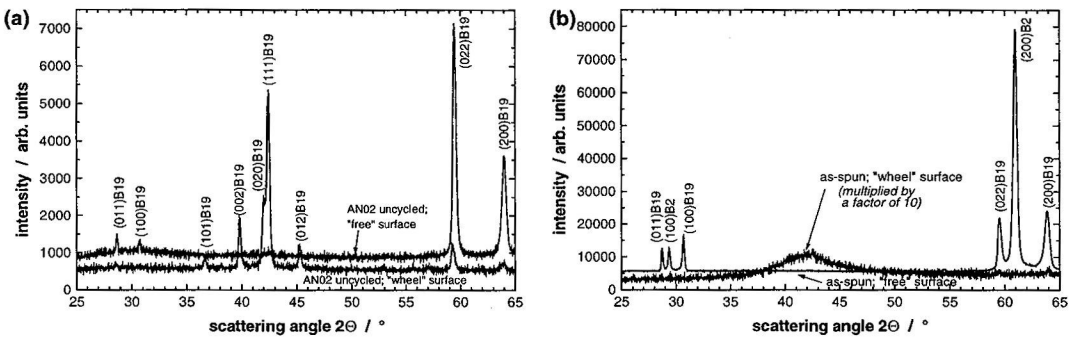


Figure 4: XRD profile of the crystallized and uncycled specimen "AN02" (a) and the as-spun reference material (b), i.e. without any heat treatment.

Fig. 4(b) displays the corresponding XRD profiles of the as-spun ribbon again from both surfaces. The "wheel" surface which experiences the fastest cooling rate during the melt spinning process is almost entirely amorphous giving rise to a broad intensity maximum around a scattering angle of 42° with solely some very small crystalline peaks at higher scattering angles. On the contrary, the X-ray profile of the "free" surface exhibits (100) and (200) peaks of as well B2 as B19 as already seen for the crystallized material [cf. Fig. 4(a)] together with $(011)_{B19}$ and $(022)_{B19}$. Evaluation of the B2 peaks leads to a lattice constant of a $B2 = 0.3038$ nm. The texture of the B19 grains is different compared to the crystallized ribbon plotted in Fig. 4(a). No evidence of an amorphous fraction in the surface layer can be detected.

In order to demonstrate the connection between the crystalline surface layer and the occurrence of two DSC peaks in cooling and (sometimes) in heating, a piece of ribbon "AN02" cycled for $N=100$ was selected. The DSC curves were measured of which the second heating and cooling cycles are plotted in Fig. 5. Thereafter, the ribbon was mechanically ground from the "free" surface side to remove the crystalline surface layer and, again, the transformation behavior was investigated by DSC and the data plotted in Fig. 5. Before mechanical grinding "AN02" clearly exhibits two peaks as well in cooling as in heating. After removing the surface layer the smaller peak on the high-temperature side is disappeared in cooling as well as in heating. Only the position of the martensitic transformation peak was shifted upwards by about 3.5°C .

Therefore, the observed two-peak transformation behavior of thermally cycled and also uncycled melt-spun ribbons after a crystallization heat treatment at 500°C for 300 s can be directly connected to the presence of a surface layer which transforms at slightly different temperatures. While working on another type of $\text{Ti}_{50}\text{Ni}_{25}\text{Cu}_{25}$ (at.%) melt-spun ribbons with different dimensions and production parameters the two-peak martensitic transformation was observed after a heat treatment at 600°C for 600 s [Fig. 6(a)]. By increasing the temperature of the heat treatment leading to a recrystallization of the surface layer the second peak could be removed. Fig. 6(b) displays the DSC curve for a heat treatment at 800°C for 600 s. A slight shoulder on the high-temperature side of the martensitic transformation peak is still visible at a temperature of 700°C (not shown due to lack of space). After $800^\circ\text{C}/600$ s this shoulder has completely disappeared [Fig. 6(b)].

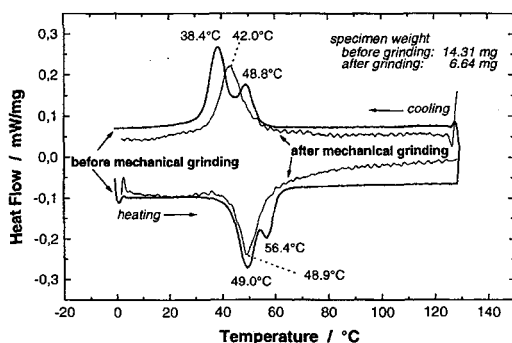


Figure 5: DSC profiles of specimen "AN02" after thermal cycling for 100 cycles before and after removing the surface layer by mechanical grinding.

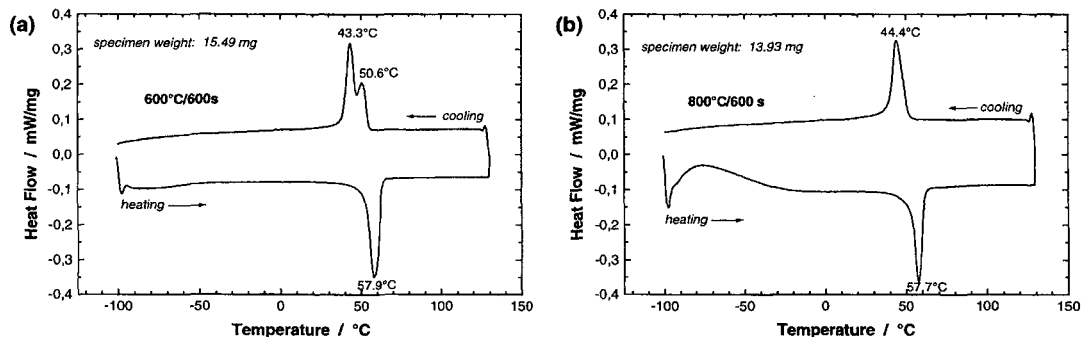


Figure 6: DSC profile of a different $\text{Ti}_{50}\text{Ni}_{25}\text{Cu}_{25}$ (at.%) melt-spun ribbon after heat treatments at 600°C (a) and 800°C (b) for 600 s; the two-peak martensitic transformation clearly discernible in (a) has completely disappeared in (b).

3.3 Microstructural characterization by TEM

The composition was found to be the nominal one within the experimental error by energy-dispersive X-ray analysis in a Scanning Electron Microscope. Specimens of ribbons "AN09" cycled for N=100 and also uncycled and of ribbon "AN07" cycled for N=5230 were investigated by TEM. All specimens exhibit the martensitic structure in agreement with the DSC results. Before knowing the nature of the second DSC peak the occurrence of R-phase was assumed as hypothesis. In-situ TEM heating and cooling experiments, however gave no evidence for the R-phase.

All ribbons investigated exhibit the same microstructure. The average grain size is about 500 nm. Twins are frequently observed in the martensitic grains. A few thin plate-like precipitates inside the matrix grains are found at higher magnifications and are assumed to be of the same nature as those recently observed in a similar melt-spun ribbon [6]. No dislocations are detected not even in the ribbon "AN07" cycled for N=5230. Since the applied stress of 50 MPa is rather low a microstructure free of dislocation is reasonable.

4. CONCLUSIONS

The conclusions of the presented work can be summarized as follows:

- Current-driven thermal cycling under an applied stress of 50 MPa does not effect the transformation behavior even after more than 5000 cycles. Only a slight peak broadening is observed by DSC.
- A crystalline surface layer, sometimes present in as-spun state of a melt-spun ribbon, leads to a second peak during DSC measurements. Crystallization at 500°C for about 300 s in vacuum is not enough to recrystallize this layer completely. A heat treatment of about 700°C for 600 s is necessary to get rid of the surface layer.
- The microstructure is not influenced by current-driven thermal cycling under an applied stress of 50 MPa.

Acknowledgments

The authors are grateful to Uta Schanz for TEM specimen preparation and the entire photographic work and to Petra Willing for the DSC measurements. Moreover, we would like to thank the Deutsche Forschungsgemeinschaft (DFG) which supported part of the presented work under contract SCHL 436/1-2.

References

- [1] A.V. Shelyakov, V.A. Antonov, Yu.A. Bykovsky, and Hodgson, N.M. Matveeva, in Proceedings of the First International Conference on Shape Memory and Superelastic Technologies (SMST-97), Asilomar, 1994, edited by A. Pelton, D. Hodgson, and T. Duerig (MIAS, Monterey, 1995), p. 335.
- [2] A.V. Shelyakov, N.M. Matveeva, and S.G.Larin, in Shape Memory Alloys: Fundamentals, Modeling and Industrial Applications, edited by F.Trochu and V.Brailovski, Canadian Inst. of Mining, Metallurgy and Petroleum, 1999, p.295.
- [3] M. Pozzi, and G. Airoidi, in Proceedings of the International Conference on Martensitic Transformations (ICOMAT-98), San Carlos de Bariloche, 1998, edited by M. Ahlers, G. Kostorz and M. Sade, Mater. Sci. Eng. A 273-275 (1999), p. 300.
- [4] G. Airoidi, G. Gomasasca and L. Omodei, in Proceedings of the First European Conference on Shape Memory and Superelastic Technologies (SMST-99), Antwerp, 1999, edited by W.F.M. Van Moorlegem (in print).
- [5] G. Gomasasca, G. Airoidi and A.V. Shelyakov, (this conference).
- [6] H. Rösner, A.V. Shelyakov, A.M. Glezer, K. Feit, and P. Schloßmacher, in Proceedings of the International Conference on Martensitic Transformations (ICOMAT-98), San Carlos de Bariloche, 1998, edited by M. Ahlers, G. Kostorz and M. Sade, Mater. Sci. Eng. A 273-275 (1999), p. 733.